A nanometer notch filter with high rejection and throughput

P. G. Carolan, A. C. Selden, C. A. Bunting, and P. Nielson

Citation: Rev. Sci. Instrum. **63**, 5161 (1992); doi: 10.1063/1.1143467
View online: http://dx.doi.org/10.1063/1.1143467
View Table of Contents: http://rsi.aip.org/resource/1/RSINAK/v63/i10
Published by the American Institute of Physics.

A nanometer notch filter with high rejection and throughput

P. G. Carolan, A. C. Selden, and C. A. Bunting
AEA Fusion, Culham Laboratory, Abingdon (UKAEA/Euratom Fusion Association), Oxon OX14 3DB, United Kingdom

P. Nielson
JET Joint Undertaking, Abingdon, Oxon OX14 3EA, United Kingdom

(Presented on 19 March 1992)

The superior *etendu* available from a Fabry–Perot spectrometer is also accessible when used in reflective mode in producing a narrow bandwidth rejection, or "notch," filter. We consider the instrumental defects and the practical effects involved in realizing a useful device. A simple figure of merit is obtained which allows the Fabry–Perot characteristics to be specified according to the desired performance of the rejection filter. A comparison is made between calculations and a prototype Fabry–Perot notch filter.

I. INTRODUCTION

There are many applications in the fusion physics program, ranging from scattering experiments to passive spectroscopy, where there are strong interfering spectral line(s). Our immediate requirement (4° forward scattering of ruby laser light), is for $\approx 10^6$ rejection at the ruby laser wavelength, ($\lambda_L = 694.3$ nm), and $>50\%$ transmission within ~ 0.5 nm of λ_L and a throughput beam product of $f/50 \times 1$ cm. Dielectric filters are available with $\sim 10^6$ attenuation but with bandwidths of $\gtrsim$ 10 nm, too broad in the context of forward scattering. Absorption filters of the same material as the lasing medium can offer considerably less than 10-nm bandwidth;[1,2] in the case of ruby, the presence of two adjacent absorption lines (R1 and R2) limits the bandwidth to a few nanometers.

Rejection based on grating spectrometers[3] can also be used but with a much lower throughput than available from amplitude division devices, such as Fabry–Perots, for much the same reasons as underlie the superior light collection capabilities, or *etendu*, of the latter when using these devices in the conventional spectrometer mode.[4]

Here we consider how a real Fabry–Perot would function in reflective mode where practical effects have a much greater impact on the instrumental performance than when used in the conventional transmission mode where the reduction of spectral resolution is of more concern than the associated small reduction in peak transmission. In making the interferometer act as a notch filter, reductions in the peak transmission translate to increases in the reflected intensity at the notch wavelength which is of more significance than the (small) accompanying increase in the notch bandwidth.

A simple figure-of-merit is used which determines the level of defects that must not be exceeded to achieve the desired rejection ratio. A comparison is made between the expected and the observed performance of the Fabry–Perot etalons immediately available to us.

II. RESPONSE OF A REAL FABRY–PEROT SYSTEM

The transmission of a Fabry–Perot includes the familiar Airy function (cf., e.g., Ref. 5) and is given by

$$T(\psi) = \Phi \left(1 - \frac{\mathscr{A}}{1-\mathscr{R}}\right)^2 \frac{1}{1 + (4\mathscr{F}_E^2/\pi^2)\sin^2(\frac{1}{2}\psi)},$$

where (cf., e.g., Ref. 6)

$$\Phi \sim 1 - \frac{2}{3}\left(1 - \frac{\mathscr{F}_E}{\mathscr{F}_{\mathscr{R}}}\right),$$

and the combined, or effective, finesse $\mathscr{F}_E$ is obtained from

$$\frac{1}{\mathscr{F}_E^2} \equiv \frac{1}{\mathscr{F}_{\mathscr{R}}^2} + \frac{1}{\mathscr{F}_D^2} + \frac{1}{\mathscr{F}_A^2},$$

and where ψ is the relative phase shift through the Fabry–Perot, $\mathscr{F}_{\mathscr{R}}$ is the familiar reflectivity finesse, $= \pi\mathscr{R}^{1/2}/(1-\mathscr{R})$, and $\mathscr{R}$ and $\mathscr{A}$ are the plate reflectivity and absorptivity. The nomenclature of finesse is also applied to the smearing arising from plate defects (e.g., irregularities, distortions, and misalignments) and finite solid angle illumination. The finesse in these cases is defined as $2\pi/\Delta\phi_{\mathrm{FWHM}}$, where $\Delta\phi_{\mathrm{FWHM}}$ is the full width at half maximum of the smearing of the phase introduced by these practical effects. Descriptions of the various forms to the plate defect finesse, $\mathscr{F}_D$, can be found in, for example, Ref. 7. It can be easily shown that the "aperture" finesse, $\mathscr{F}_A$, due to finite solid angle axial illumination, is given by

$$\mathscr{F}_A(0) \sim \frac{3}{\alpha^2}\frac{\Delta\lambda_{\mathrm{FSR}}}{\lambda},$$

where α is the half apex angle of the input cone of wave vectors, $\Delta\lambda_{\mathrm{FSR}}$ is the free spectral range, $= \Delta\lambda_{\mathrm{FSR}} = \lambda^2/2s$, and s is the optical spacing of the plates. For our values of $\sim f/100$ aperture (i.e., $\alpha = 1/200$), $\Delta\lambda_{\mathrm{FSR}} = 14$ nm, and $\lambda = 694$ nm, we have $\mathscr{F}_A \approx 2 \times 10^3$ and so the small solid angle used makes only a negligible contribution to $\mathscr{F}_E$ for axial illumination. Thus, the finesses $\mathscr{F}_{\mathscr{R}}$ and $\mathscr{F}_{\mathscr{R}D}$ can be obtained directly from the measured (effective) finesse and the peak transmission and $\Delta\lambda_{\mathrm{FSR}}$ of the transmission response functions.

Armed with the measurements of the various finesses we can calculate the rejection factor of the Fabry–Perot used in reflective mode. Taking proper account of how

 0034-6748/92/105161-03$02.00

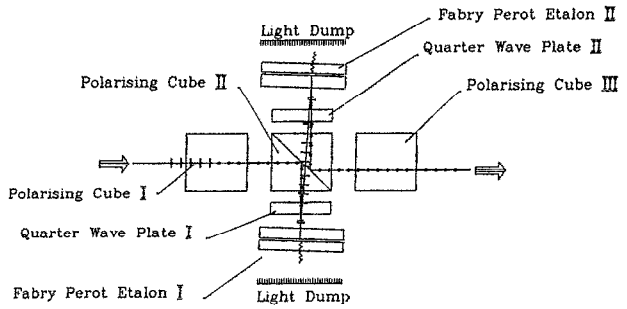

FIG. 1. Schematic of a module of two Fabry–Perot étalons used in reflection mode. (●) represents polarization perpendicular to the plane of the diagram.

absorption affects the reflected intensity[8] it can be shown that the minimum $\rho_{\min}$ in reflected intensity is given by

$$\rho_{\min}\sim\frac{1}{3}\left(\frac{\mathscr{F}_{\mathscr{R}}^2}{\mathscr{F}_A^2}+\frac{\mathscr{F}_{\mathscr{R}}^2}{\mathscr{F}_D^2}\right)+\frac{\mathscr{R}\mathscr{A}^2}{(1-\mathscr{R})^2}.$$

The last term is negligible in our conditions and so to maximize the rejection ratio of the filter it is desirable that $\mathscr{F}_A^2 \gg \mathscr{F}_{\mathscr{R}}^2$. This results in a simple figure-of-merit for the lowest defect finesse, $\mathscr{F}_D$, acceptable for the rejection ratio desired, i.e.,

$$\mathscr{F}_D^2 > \frac{\mathscr{F}_{\mathscr{R}}^2}{3\rho_{\min}}.$$

III. DESCRIPTION OF TEST APPARATUS

A single, medium-sized, Fabry–Perot ($\sim$75-mm diameter) with high quality plates ($\sim\lambda/200$) can be incorporated into a recycling optics arrangement which presents the reflected light several times to the Fabry–Perot, at separate regions of the plates, and so greatly enhances the attenuation at the notch wavelength. Such a Fabry–Perot, with the appropriate free spectral range and plate spacing stability, was not immediately available to us, so we investigated the possibility of using instead a train of small fixed etalons.[9] However, although surprisingly good quality étalons can be procured as standard items at relatively low cost,[10] the plate defects and misalignments are understandably larger than available in fully adjustable Fabry–Perot interferometers. Small angular tilts, ($\lesssim 2°$) can compensate for the peak transmissions occurring at slightly different wavelengths, $\lesssim$0.4 nm greater than our desired $\lambda_L = 694.3$ nm). Operation in a temperature-stable environment is, of course, mandatory.

A modular two Fabry–Perot system is shown schematically in Fig. 1. The functions of the elements are as follows: The incoming light is plane polarized by Polarizing Cube I and is then reflected by the second cube to the $\lambda/4$ plate; the reflected light from the Fabry–Perot is plane polarized on passing, for the second time, through the $\lambda/4$ plate; the light, now polarized perpendicular to the original, is transmitted by the cube to the next Fabry–Perot stage; the returned light is polarized in the original direction and is therefore reflected by the polarizing cube. The function of Polarizing Cube III is to remove residual perpendicular components of polarization and to present high attenuation for light trying to pass directly through the system.

Since each pair of Fabry–Perots is self-contained, we can adjust each module separately before bringing them together as a complete unit. We first ensure the input light is well collimated using a 1-mm-diam fiber at the focal plane of a 100-mm camera lens. The input of the fiber is irradiated by a tungsten lamp. The orientation of the polarizing cubes and the $\lambda/4$ plates is first achieved by conventional means (e.g., seeking maximum extinction using crossed polarizers). The alignment of the Fabry–Perot elements consists of adjusting the first one, substituting the second with a mirror, while the output is transmitted to a spectrometer (1.25-m grating instrument with $\sim$0.35 nm/mm inverse dispersion). When the desired notch wavelength is obtained, the second Fabry–Perot is installed and the adjustments repeated. The problem of vignetting is considered when making choices of which plane of the Fabry–Perot unit to adjust when tuning to the notch wavelength. The tilt of one Fabry–Perot can be compensated, at least partly, by the next in series by tilting in the opposite direction when adjusting for the wavelength offset. Also, making the complete device as compact as possible is important in limiting the overall vignetting (e.g., the complete optical length of our present device is $\sim$35 cm from the front input face of the first cube to the output of the last cube).

IV. TRANSMISSION PERFORMANCE OF ÉTALONS

The transmission response functions of the Fabry–Perot étalons were measured using axial illumination of $f/100$ and 2-cm beam diameter light. The transmitted light is imaged at the entrance slit of a 1.25-m spectrometer with a slit-width bandwidth of, typically, 0.02 nm and much smaller than the Fabry–Perot $\Delta\lambda_{\mathrm{FWHM}}$. Three of the étalons had acceptable central wavelengths but, unfortunately, it was difficult to incorporate the fourth owing to the large tilt required and the consequent vignetting. The typical measured $\Delta\lambda_{\mathrm{FWHM}}$ is somewhat larger than that expected from the reflectivity finesse; the expected $\mathscr{F}_{\mathscr{R}}\sim 38$, for ($\mathscr{R}=92\%$), and the free spectral range of $\Delta\lambda_{\mathrm{FSR}}\sim 14$ nm would together give a $\Delta\lambda_{\mathrm{FWHM}}\sim 0.37$ nm. These compare with the measured, or "effective," finesse of $\mathscr{F}_E\sim 29$ and a $\Delta\lambda_{\mathrm{FWHM}}\sim 0.5$ nm. The associated underlying "defect" finesse is $\mathscr{F}_D\sim 44$. This defect finesse is too low to allow for better than a 15% rejection ratio of the input intensity to be reflected at the notch wavelength. We need $\mathscr{F}_D \geqslant 130$ to achieve 10^6 attenuation in four stages (i.e., $\rho_{\min}\leqslant 0.03$ per etalon) for the chosen $\mathscr{F}_{\mathscr{R}}$ and $\Delta\lambda_{\mathrm{FSR}}$. While this plate quality can be achieved, at some cost, for more conventional Fabry–Perots, it transpired to be much more difficult for these more compact étalons.

V. COMPUTATIONAL RESULTS

We simulate the reflected response functions from the measured transmission characteristics and the calculated

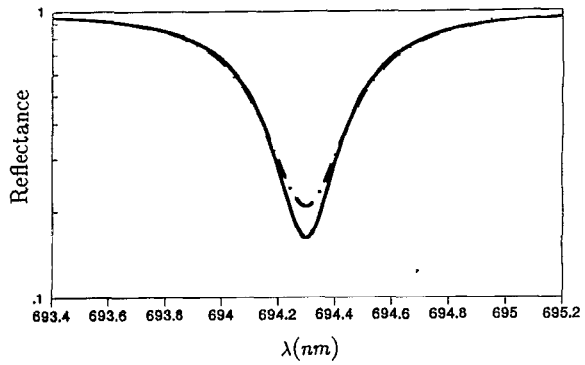

FIG. 2. Calculation of the expected reflected response function of two Fabry–Perots, one with zero tilt and the other with a tilt of 2° to accommodate a shift of ~0.4 nm in axial wavelength. Measured effects of plate defects are included in the calculations.

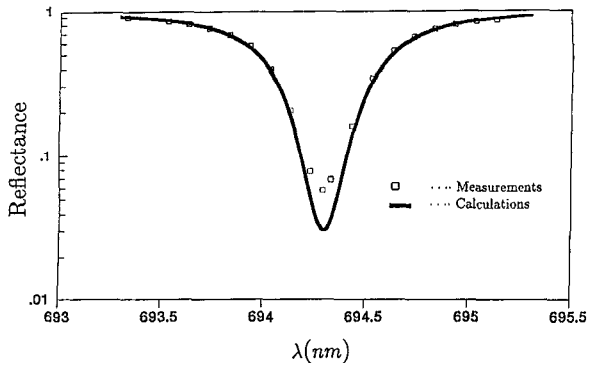

FIG. 3. Comparison between the observed and calculated reflected functions of two Fabry–Perots used in tandem. Measured tilts, plate defects, solid angle illumination, together with the reflectivity absorption of the plates, are included in the calculations.

reflectivity finesse. The measured finesse, $\mathcal{F}_E$, is used to obtain the defect finesse, $\mathcal{F}_D$, which is then included in calculating the reflected response function. We obtain, for perpendicular illumination and small input divergence, a maximum transmission $T_{\max} \sim 80\%$ and a minimum intensity in the reflected response function of $\sim 15\%$ with the remaining $\sim 5\%$ absorbed (coating absorptivity $\sim 0.2\%$). The $\sim 15\%$ rejection ratio is much larger than that expected from error free plates, even with the finite divergence of light used here ($< 0.1\%$ for $f/100$). In general, it is necessary to tilt the étalons since their central wavelengths can differ from the desired notch wavelength. The consequence is that the "aperture" finesse is reduced and so diminishing the rejection ratio at the notch wavelength, particularly for high finesse systems.

In Fig. 2 we show a comparison between two calculated reflection response functions for a Fabry–Perot with no tilt and the other tilted to accommodate a 0.4-nm shift from the notch wavelength at 694.3 nm. We incorporate the measured $\mathcal{F}_E$ and the finite input cone illumination. The small difference in the response functions illustrates the dominating effect of the plate defects in the present etalons.

VI. COMPARISON BETWEEN CALCULATED AND OBSERVED REFLECTED RESPONSE FUNCTIONS

A single Fabry–Perot arrangement typically gives an intensity at the notch wavelength which is $\approx 15\%$ that of intensities well outside the notch. This is also what we find from the above formulations and gives us some confidence in our treatment, especially the role of plate defects. Combining two Fabry–Perots in a single module we show in Fig. 3 the comparison between observation and calculations. The computations take account of the tilt required to match the Fabry–Perots to the same notch wavelength. In this application the notched intensity is $\sim 6\%$ of input and good agreement is found between simulations and measurements of the reflected response function. The source(s) of the difference between the measured and calculated rejection ratio ($\sim 16{:}1$ and $\sim 33{:}1$, respectively) has not been clearly identified and could be due to internal reflections, slight temperature changes affecting the plate spacing, and alignment occurring after the transmission measurements were collected, or that our portrayal of plate defects is not representative enough of the true defects, if indeed they are at all sufficiently measurable (cf., e.g., Ref. 7 for the contribution of the different types of plate defects). Future attempts will pay greater attention to eliminating sources of stray light affecting the minimum intensity at the notch wavelength. Nevertheless, considering that the reflected intensity is obtained by subtracting from unity numbers that are very close to unity so that small errors will have a large effect, our modeling of rejection ratio compares well with the experimental results.

Combining three Fabry–Perots gave a $\sim 1\%$ notch effect, as expected from our formulations and experience with the two Fabry–Perot system. Therefore, the best we could reasonably expect from our present four-étalon system, with an acceptable fourth étalon, is a notch intensity at 2×10^{-3} of the input intensity at that wavelength, i.e., 500:1 rejection ratio.

In our case, *reducing* the $\mathcal{F}_{\mathscr{R}}$ by, say, a factor of 2 would increase the notch bandwidth to ~ 2 nm but enhance the rejection factor to $\gtrsim 10^5$, where the accompanying aperture of $\sim f/20$ is more than adequate for most purposes. However, greater attention would probably have to be given to residual effects, such as internal reflections, to achieve such high rejection.

[1] C. E. Thomas, Jr., E. A. Lazarus, R. R. Kindsfather, *et al.*, Rev. Sci. Instrum. **57**, 1819 (1986).
[2] C. W. Gowers, K. Hirsch, P. Nielsen, and H. Salzmann, Appl. Opt. **27**, 17 (1988).
[3] R. E. Siemon, Appl. Opt. **13**, 697 (1974).
[4] P. Jacquinot, J. Opt. Soc. Am. **44**, 761 (1954).
[5] M. Born and E. Wolf, *Principles of Optics*, 6th ed. (Pergamon, Oxford, 1983).
[6] W. H. Steel, *Interferometry*, 2nd ed. (Cambridge University, 1983).
[7] J. M. Vaughan, *The Fabry–Perot Interferometer* (Adam Hilger, 1989).
[8] J. Holden, J. Proc. Phys. Soc. B **62**, 405 (1949).
[9] M. A. Mahdavi, Rev. Sci. Intrum. **47**, 56 (1976).
[10] Technical Optics Limited, Onchen, Isle of Man, United Kingdom.